ADDED MASS EFFECTS ON INTERNAL WAVE GENERATION

BRUNO VOISIN

Laboratoire des Écoulements Géophysiques et Industriels,
CNRS, UJF, INPG; BP 53, 38041 Grenoble, France
E-mail: bruno.voisin@hmg.inpg.fr

Abstract. A representation is proposed for the small oscillations of bodies in unbounded uniformly stratified Boussinesq fluids, in terms of a surface distribution of singularities. The distribution satisfies an integral equation, expressing the continuity of normal velocity. The equation is solved for a sphere and a circular cylinder; when these are rigid, the form of the distribution is interpreted in terms of added mass.

In a stratified fluid, owing to the generation of internal waves by vertical motion (propagating waves at frequencies below the buoyancy frequency, evanescent waves at frequencies above it), added mass becomes anisotropic and frequency-dependent. It is only in the limit of large frequencies that the coefficients of added mass in a homogeneous fluid, $1/2$ for the sphere and 1 for the circular cylinder, are recovered. Two definitions of added mass are considered, based on the impulse of the fluid and on the pressure on the body, respectively. In a homogeneous fluid they are equivalent; stratification makes them distinct, leading to two different forms of added mass.

Two applications are considered: the wave power radiated by the forced oscillations of a body; and the free oscillations of a body displaced from its equilibrium level then released. A maximum of the wave power is observed at a practically constant fraction 0.8 of the buoyancy frequency, and its implications for the radiation of waves from regions of random fluid motion are discussed.

1. Introduction

Owing to realization of the importance of internal tides in ocean dynamics[1] and to successful reproduction of these tides in the laboratory using oscillatory flow over topography,[2] the classical problem of the generation of internal waves by oscillating objects is experiencing renewed interest. As a consequence, the objects used in the laboratory have gained increasing sophistication, from classical oscillating cylinders[3–5] and spheres[6] to innovative paddles.[7] The present paper studies the modelling of bodies oscillating with small amplitude in unbounded uniformly stratified Boussinesq fluids, using a sphere and a circular cylinder as three- and two-dimensional examples, respectively. For rigid bodies, the models are linked with the modification of the added mass of the bodies by the stratification.

2. Wave Generation

The problem and notations are illustrated in Fig. 1. In a fluid of density $\rho_0(z)$ at rest and constant buoyancy frequency $N = [-(g/\rho_0)(\mathrm{d}\rho_0/\mathrm{d}z)]^{1/2}$, with z the upward vertical coordinate and g the acceleration due to gravity, a body of volume V has the distribution of velocity $\mathbf{U}(\mathbf{x})\mathrm{e}^{-\mathrm{i}\omega t}$ imposed at its surface S. The motion of the fluid is described in terms of a wave function χ,[8] satisfying the wave equation

$$\left(\frac{\partial^2}{\partial t^2}\nabla^2 + N^2\nabla_\mathrm{h}^2\right)\chi(\mathbf{x}, t) = 0, \tag{1}$$

with boundary condition

$$\left(\frac{\partial^2}{\partial t^2}\frac{\partial}{\partial n} + N^2\frac{\partial}{\partial n_\mathrm{h}}\right)\chi(\mathbf{x}, t) = U_n(\mathbf{x})\mathrm{e}^{-\mathrm{i}\omega t} \quad \text{for } \mathbf{x} \in S, \tag{2}$$

where the subscript h denotes a horizontal projection and $\mathbf{n}$ the outward normal to S. The disturbances in pressure p, velocity $\mathbf{u}$ and density ρ follow as

$$p = -\rho_0\left(\frac{\partial^2}{\partial t^2} + N^2\right)\frac{\partial\chi}{\partial t}, \quad \mathbf{u} = \left(\frac{\partial^2}{\partial t^2}\nabla + N^2\nabla_\mathrm{h}\right)\chi, \quad \rho = \rho_0\frac{N^2}{g}\frac{\partial^2\chi}{\partial t\partial z}. \tag{3}$$

All quantities depend on time through the factor $\mathrm{e}^{-\mathrm{i}\omega t}$ which is suppressed in the following, so that $\partial/\partial t \equiv -\mathrm{i}\omega$.

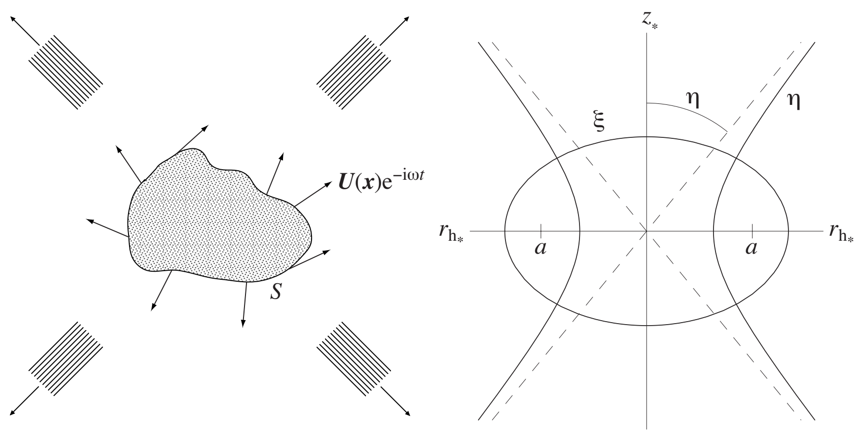

Figure 1. Generation of waves by an oscillating object (left) and oblate spheroidal coordinates (right).

We replace the boundary forcing by a source term $q(\mathbf{x}) = \sigma(\mathbf{x})\delta_S(\mathbf{x})$ in the wave equation, distributing singularities with density σ along S, where δ_S is the

Dirac delta function of support S. Convolution with the Green's function[8] of the wave equation yields the wave function

$$\chi(\mathbf{x}) = \frac{1}{4\pi(\omega^2 - N^2)^{1/2}} \oint_S \frac{\sigma(\mathbf{x}')}{[\omega^2(\mathbf{x}-\mathbf{x}')^2 - N^2(z-z')^2]^{1/2}} \, \mathrm{d}^2 S', \tag{4}$$

transforming the boundary condition into an integral equation for σ, namely

$$U_n(\mathbf{x}) = -\frac{1}{4\pi(\omega^2 - N^2)^{1/2}} \left(\omega^2 \frac{\partial}{\partial n} - N^2 \frac{\partial}{\partial n_{\mathrm{h}}}\right) \times \oint_S \frac{\sigma(\mathbf{x}')}{[\omega^2(\mathbf{x}-\mathbf{x}')^2 - N^2(z-z')^2]^{1/2}} \, \mathrm{d}^2 S' \quad \text{for } \mathbf{x} \in S. \tag{5}$$

One advantage of this procedure, introduced for lee waves[9] and applied later to monochromatic waves,[10,11] is that once the representation of the forcing is known it is straightforward to incorporate additional effects into the analysis, such as viscosity,[12] unsteadiness and near field, as is required for comparison with experiment.[13] Until now, for the two most popular internal wave generators, a rigid cylinder[14–16] and a rigid sphere,[6] people have resorted instead to solving first the steady inviscid problem (1)–(2), then deducing the spectrum of the forcing from the solution, and finally adding viscous effects.

2.1. *Oscillating sphere*

We consider first a sphere of radius a. For $\omega > N$, stretching the coordinates anisotropically according to

$$x = \frac{N}{\omega} x_\star, \quad y = \frac{N}{\omega} y_\star, \quad z = \frac{N}{(\omega^2 - N^2)^{1/2}} z_\star, \tag{6}$$

transforms the kernel of the integral equation into the Poisson kernel $1/|\mathbf{x}_\star - \mathbf{x}'_\star|$ and the sphere into an oblate spheroid, dictating the introduction of the appropriate spheroidal coordinates (ξ, η, ϕ),[17] defined by

$$x_\star = a \cosh\xi \sin\eta \cos\phi, \quad y_\star = a \cosh\xi \sin\eta \sin\phi, \quad z_\star = a \sinh\xi \cos\eta, \tag{7}$$

and illustrated in Fig. 1. The pseudo-radial coordinate ξ and the pseudo-angular coordinate η are constant on confocal spheroids and hyperboloids, respectively.

On the sphere, $\xi = \xi_0 = \operatorname{arccosh}(\omega/N)$ and $\eta = \theta$ with θ the colatitude. Equation (5) reduces to a standard integral equation,

$$U_r(\theta, \phi) = -\frac{a}{4\pi} \frac{\omega}{N} \frac{\partial}{\partial \xi} \oint_{\xi'=\xi_0} \frac{\sigma(\theta', \phi')}{|\mathbf{x}_\star - \mathbf{x}'_\star|} \, \mathrm{d}^2\Omega' \quad \text{at } \xi = \xi_0, \tag{8}$$

with $\mathrm{d}^2\Omega' = \sin\theta'\mathrm{d}\theta'\mathrm{d}\phi'$ the elementary solid angle, and is solved by expansion in spherical harmonics Y_{lm}.[18] We write

$$U_r(\theta,\phi) = \sum_{l=0}^{\infty}\sum_{m=-l}^{l} U_{lm} Y_{lm}(\theta,\phi), \tag{9}$$

and use[19]

$$\frac{a}{|\mathbf{x}_\star - \mathbf{x}'_\star|} = 4\mathrm{i}\pi \sum_{l=0}^{\infty}\sum_{m=-l}^{l} (-1)^m \frac{(l-m)!}{(l+m)!} \times P_{lm}(\mathrm{i}\sinh\xi_<) Q_{lm}(\mathrm{i}\sinh\xi_>) Y_{lm}(\eta,\phi)\overline{Y_{lm}}(\eta',\phi'), \tag{10}$$

where P_{lm} and Q_{lm} are associated Legendre functions, $\xi_<$ ($\xi_>$) is the smaller (larger) of ξ and ξ', and a bar $^-$ denotes a complex conjugate. We obtain

$$\sigma(\theta,\phi) = \frac{N^2}{\omega^2}\sum_{l=0}^{\infty}\sum_{m=-l}^{l} (-1)^m \frac{(l+m)!}{(l-m)!} U_{lm} \frac{Y_{lm}(\theta,\phi)}{P_{lm}(\mathrm{i}\sinh\xi_0) Q'_{lm}(\mathrm{i}\sinh\xi_0)}, \tag{11}$$

and simultaneously

$$p(\mathbf{x}) = \rho_0 N a \left(1 - \frac{N^2}{\omega^2}\right)^{1/2} \sum_{l=0}^{\infty}\sum_{m=-l}^{l} U_{lm} \frac{Q_{lm}(\mathrm{i}\sinh\xi) Y_{lm}(\eta,\phi)}{Q'_{lm}(\mathrm{i}\sinh\xi_0)}. \tag{12}$$

The solution is then extended to frequencies $0 < \omega < N$ by analytic continuation onto the upper half of the complex ω-plane, in accordance with causality.[20]

When the sphere is rigid, only the dipolar terms, corresponding to $l = 1$, contribute to the expansion. The equivalent source,

$$q(\mathbf{x}) = \frac{3}{2}\mathbf{U}^\star \cdot \frac{\mathbf{x}}{a}\delta(r-a), \tag{13}$$

with $r = |\mathbf{x}|$, is identical to that in a homogeneous fluid except for the replacement of the actual velocity $\mathbf{U}$ by the virtual velocity $\mathbf{U}^\star$, such that

$$\mathbf{U}^\star_\mathrm{h} = \frac{4/3}{1+A}\mathbf{U}_\mathrm{h}, \quad U^\star_z = \frac{2/3}{1-A}U_z, \tag{14}$$

with

$$A(\omega) = \frac{\omega^2}{N^2}\left[1 - \left(\frac{\omega^2}{N^2} - 1\right)^{1/2} \arcsin\left(\frac{N}{\omega}\right)\right], \tag{15}$$

becoming, for $0 < \omega < N$,

$$A(\omega) = \frac{\omega^2}{N^2}\left[1 - \left(1 - \frac{\omega^2}{N^2}\right)^{1/2} \operatorname{arccosh}\left(\frac{N}{\omega}\right) - \mathrm{i}\frac{\pi}{2}\left(1 - \frac{\omega^2}{N^2}\right)^{1/2}\right]. \tag{16}$$

In the limit $\omega/N \to \infty$ the influence of the stratification vanishes, with $A \to 1/3$ and $\mathbf{U}^\star \to \mathbf{U}$.

2.2. *Oscillating circular cylinder*

The case of a horizontal circular cylinder of radius a is treated in the same way, using elliptical coordinates instead of spheroidal coordinates.[21] Again, when the cylinder is rigid, the equivalent source,

$$q(\mathbf{x}) = 2\mathbf{U}^\star \cdot \frac{\mathbf{x}}{a}\delta(r-a), \tag{17}$$

is identical to that in a homogeneous fluid except for the replacement of $\mathbf{U}$ by $\mathbf{U}^\star$, such that

$$U_\mathrm{h}^\star = \frac{1+(1-N^2/\omega^2)^{1/2}}{2}U_\mathrm{h}, \quad U_z^\star = \frac{1+(1-N^2/\omega^2)^{-1/2}}{2}U_z. \tag{18}$$

By analytic continuation we have, for $0 < \omega < N$,

$$\left(1-\frac{N^2}{\omega^2}\right)^{1/2} = \mathrm{i}\left(\frac{N^2}{\omega^2}-1\right)^{1/2}, \tag{19}$$

and in the limit $\omega/N \to \infty$ we verify that $\mathbf{U}^\star \to \mathbf{U}$.

3. Added Mass

The replacement of the actual velocity $\mathbf{U}$ by the virtual velocity $\mathbf{U}^\star$ is a manifestation of a more general phenomenon: in a stratified fluid, the modification of the added mass of oscillating rigid bodies owing to buoyancy. For irrotational flow of a homogeneous fluid, two equivalent definitions of added mass are used indifferently in the literature, based on the impulse of the fluid and on the pressure on the body, respectively. We consider them in turn.

3.1. *Impulse-based definition*

The first definition[22,23] uses the fluid impulse $\mathbf{I}$, related to the dipole strength $\mathbf{D}$ of the body by

$$\rho_0\mathbf{D} = \rho_0 V\mathbf{U} + \mathbf{I}, \tag{20}$$

and representing the momentum which the body must communicate to the fluid to generate the motion of this fluid from rest. Owing to the linearity of the equations of motion, a linear relation exists between the fluid impulse and the velocity of the body, of the form

$$I_i = \rho_0 V C_{ij}^{(1)} U_j, \tag{21}$$

yielding a first definition of the added mass coefficients $C_{ij}^{(1)}$ and allowing their derivation from the distribution of singularities $\sigma(\mathbf{x})$, through the equation

$$D_i = \oint_S x_i \sigma(\mathbf{x})\, \mathrm{d}^2 S = V[\delta_{ij} + C_{ij}^{(1)}]U_j, \tag{22}$$

with δ_{ij} the Kronecker delta symbol.

In a stratified fluid, derivation of a Kirchhoff–Helmholtz integral equation[24,25] from the wave equation, followed by multipolar expansion, implies that Eq. (20) remains valid provided the fluid impulse is defined in terms of the wave function as

$$\mathbf{I} = \rho_0 \oint_S \left(\omega^2 \mathbf{n} - N^2 \mathbf{n}_\mathrm{h}\right) \chi(\mathbf{x})\, \mathrm{d}^2 S. \tag{23}$$

From Eq. (22) we obtain for the sphere

$$C_\mathrm{h}^{(1)} = \frac{1-A}{1+A}, \quad C_z^{(1)} = \frac{A}{1-A}, \tag{24}$$

and for the circular cylinder

$$C_\mathrm{h}^{(1)} = \left(1 - \frac{N^2}{\omega^2}\right)^{1/2}, \quad C_z^{(1)} = \left(1 - \frac{N^2}{\omega^2}\right)^{-1/2}. \tag{25}$$

The coefficients of added mass become complex and frequency-dependent. Their variations are represented in Fig. 2, in modulus and argument. As $\omega/N \to \infty$ the values in a homogeneous fluid, $C_\infty = 1/2$ for the sphere and 1 for the cylinder, are recovered.

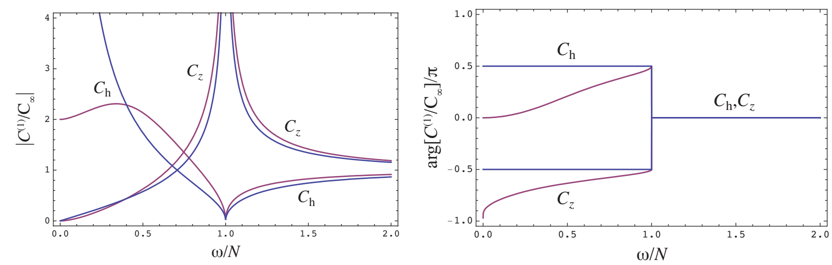

Figure 2. Impulse-based added mass coefficients of a sphere (red) and a circular cylinder (blue).

3.2. *Pressure-based definition*

The second definition[26,27] uses the hydrodynamic pressure force exerted by the fluid on the body, given by

$$\mathbf{F}_\mathrm{d} = -\oint_S \mathbf{n} p(\mathbf{x})\,\mathrm{d}^2 S. \tag{26}$$

Again, owing to the linearity of the equations of motion, a linear relation exists between this force and the acceleration of the body, of the form

$$F_{\mathrm{d}_i} = \mathrm{i}\rho_0 \omega V C_{ij}^{(2)} U_j, \tag{27}$$

yielding a second definition of the added mass coefficients $C_{ij}^{(2)}$ and allowing their derivation from the distribution of hydrodynamic pressure $p(\mathbf{x})$.

In a homogeneous fluid the two definitions are equivalent, since $-\mathbf{F}_\mathrm{d}$ is the force exerted by the body on the fluid so that $\mathbf{F}_\mathrm{d} = \mathrm{i}\omega\mathbf{I}$. In a stratified fluid the existence of an additional force, buoyancy, breaks the equivalence. Using Eq. (3) we obtain

$$\mathbf{F}_\mathrm{d} = \mathrm{i}\rho_0\omega(\omega^2 - N^2) \oint_S \mathbf{n}\chi(\mathbf{x})\,\mathrm{d}^2 S, \tag{28}$$

and comparison with Eq. (23) shows that the two definitions (21) and (27) yield different results. In particular, for the sphere and the circular cylinder we have

$$C_\mathrm{h}^{(2)} = C_\mathrm{h}^{(1)}, \quad C_z^{(2)} = \left(1 - \frac{N^2}{\omega^2}\right) C_z^{(1)}. \tag{29}$$

The resulting expressions of $C^{(2)}$ agree with previous direct calculations.[14,27]

The equation of motion of the body under an external force $\mathbf{F}_\mathrm{e}$ is[28]

$$-\rho_0 V\omega^2 \mathbf{X} = \mathbf{F}_\mathrm{d} - \rho_0 V N^2 Z \mathbf{e}_z + \mathbf{F}_\mathrm{e}, \tag{30}$$

for the position $\mathbf{X}$ of the centroid of the displaced fluid, such that $\mathbf{U} = -\mathrm{i}\omega\mathbf{X}$, relative to the equilibrium level $Z = 0$. The second term on the right-hand side represents the buoyancy of the body, namely the combination of hydrostatic pressure (Archimede's force) and weight. Separating real and imaginary parts, the equation may be recast as

$$\left\{-\frac{\omega^2}{N^2}\left[\delta_{ij} + \mathrm{Re}\, C_{ij}^{(2)}\right] - \mathrm{i}\frac{\omega}{N}\left[\frac{\omega}{N}\,\mathrm{Im}\, C_{ij}^{(2)}\right] - \delta_{i3}\delta_{j3}\right\} X_j = \frac{F_{\mathrm{e}_i}}{\rho_0 V N^2}, \tag{31}$$

validating the interpretation of $\mathrm{Re}\, C^{(2)}$ as a coefficient of added mass in the usual sense and $(\omega/N)\,\mathrm{Im}\, C^{(2)}$ as a coefficient of damping. The variations of these coefficients for the sphere and the cylinder are represented in Fig. 3, and have been verified experimentally for horizontal oscillations.[29–32]

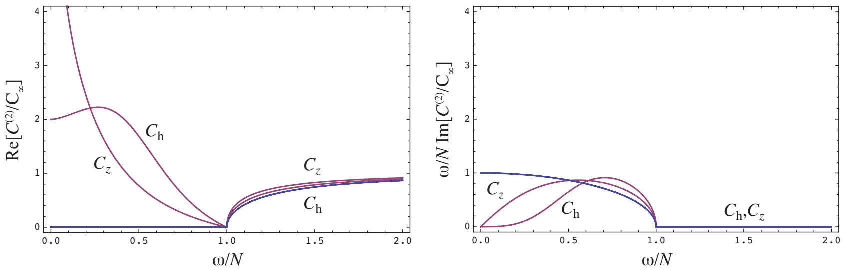

Figure 3. Pressure-based added mass coefficients of a sphere (red) and a circular cylinder (blue).

4. Applications

4.1. *Wave power*

Knowledge of the source term equivalent to an oscillating body allows straightforward derivation of the power of the waves radiated away from the body, as an integral of the source spectrum squared.[8,33] Assuming fixed amplitude R and inclination α of the oscillations to the vertical, so that $\mathbf{X} = R(\sin\alpha, 0, \cos\alpha)$, we obtain for $0 < \omega < N$, for the sphere,

$$P = \frac{\pi^2}{3}\rho_0 N^3 a^3 R^2 \frac{\omega^3}{N^3}\left(1 - \frac{\omega^2}{N^2}\right)^{1/2} \times \left[2\frac{\omega^2}{N^2}\frac{\sin^2\alpha}{|1+A|^2} + \left(1 - \frac{\omega^2}{N^2}\right)\frac{\cos^2\alpha}{|1-A|^2}\right], \qquad (32)$$

and for the circular cylinder,[14]

$$P = \frac{\pi}{2}\rho_0 N^3 a^2 R^2 \frac{\omega^2}{N^2}\left(1 - \frac{\omega^2}{N^2}\right)^{1/2}, \qquad (33)$$

while $P = 0$ for $\omega > N$. The variations of P with ω are represented in Fig. 4, and have been verified experimentally for horizontal oscillations.[30,32] A maximum is observed at $\omega_0/N = \sqrt{(2/3)} \approx 0.82$ independent of α for the cylinder, and ω_0/N varying weakly with α, between 0.84 and 0.85, for the sphere.

A tentative extrapolation relates to wave emission by assemblies of randomly moving fluid patches located in a region of space with fixed centre of mass: for such broadband excitation, if the patches are assumed to move in arbitrary directions with approximately fixed excursion, then the waves radiated away from the region are expected to have a power spectrum peaked at frequency ω_0. Such spectra have been observed experimentally for a two-dimensional mixed region released at its equilibrium level[34] ($\omega_0/N = 0.8$) or above it[35] ($\omega_0/N = 0.7$), and numerically during the decrease of three-dimensional turbulence[36] ($\omega_0/N = 0.5$).

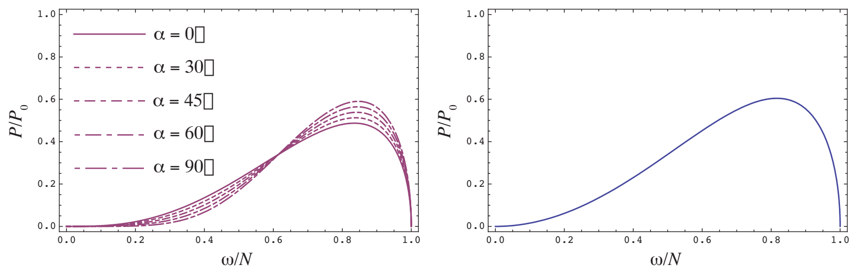

Figure 4. Wave power from a sphere (red) and a circular cylinder (blue), normalized by $P_0 = \rho_0 N^3 a^3 R^2$ for the sphere and $\rho_0 N^3 a^2 R^2$ for the cylinder.

4.2. *Buoyant release*

The variations of the vertical coefficient of added mass with frequency are related unequivocally[30] to the spectrum $Z(\omega) = \int_0^\infty Z(t)\mathrm{e}^{\mathrm{i}\omega t}\,\mathrm{d}t$ of the free oscillations $Z(t)$ of a rigid body displaced a small distance $|Z_0| \ll a$ from its equilibrium level then released at time $t = 0$. This corresponds in Eq. (31) to the application of a force $F_{\mathrm{e}_z} = \rho_0 V N^2 Z_0$ for $t < 0$ and 0 for $t > 0$, yielding

$$\frac{Z(\omega)}{Z_0} = \frac{\mathrm{i}}{\omega}\frac{C_z^{(2)}(\omega) + 1}{C_z^{(2)}(\omega) + 1 - N^2/\omega^2}. \tag{34}$$

For the sphere and the circular cylinder we obtain by Fourier inversion

$$\frac{Z(t)}{Z_0} = \frac{\pi}{2}\mathbf{H}_{-1}(Nt), \qquad \frac{Z(t)}{Z_0} = J_0(Nt), \tag{35}$$

respectively, where J_ν and $\mathbf{H}_\nu$ are Bessel and Struve functions, consistently with previous direct calculations and experimental measurements for the sphere.[28] The oscillations are represented in Fig. 5 together with their spectrum.

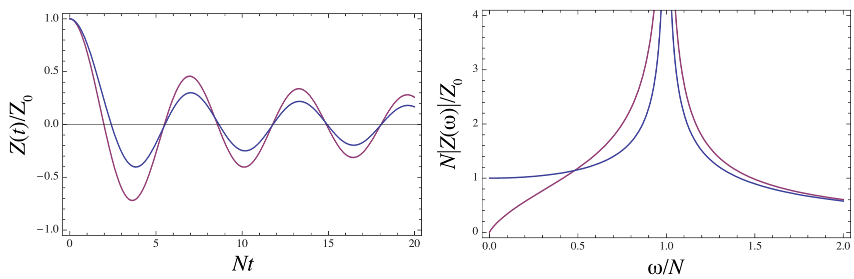

Figure 5. Free oscillations of a sphere (red) and a circular cylinder (blue).

When the initial displacement becomes comparable with the size of the body, competition arises between viscous drag and wave drag. Ultimately, as $|Z_0| \gg a$, viscosity takes over, as has been verified in the laboratory[37] and in the field.[38]

Acknowledgments

This work has been supported at DAMTP by Marie Curie fellowship 972653 in 1998, and at LEGI by a PATOM grant of the Institut National des Sciences de l'Univers in 2005 and by grant TOPOGI-3D of the Agence Nationale de la Recherche in 2006 and 2007. Benefit from conversations with Professors Valentin Gorodtsov and Yuli Chashechkin in Moscow, and Professor Izolda Sturova and Dr Evgeny Ermanyuk in Novosibirsk, is acknowledged.

References

1. C. Garrett and E. Kunze, *Annu. Rev. Fluid Mech.* **39**, 57–87 (2007).
2. L. Gostiaux and T. Dauxois, *Phys. Fluids* **19**, 028102 (2007).
3. B. R. Sutherland, S. B. Dalziel, G. O. Hughes and P. F. Linden, *J. Fluid Mech.* **390**, 93–126 (1999).
4. B. R. Sutherland, G. O. Hughes, S. B. Dalziel and P. F. Linden, *Dyn. Atmos. Oceans* **31**, 209–232 (2000).
5. B. R. Sutherland and P. F. Linden, *Phys. Fluids* **14**, 721–731 (2002).
6. M. R. Flynn, K. Onu and B. R. Sutherland, *J. Fluid Mech.* **494**, 65–93 (2003).
7. L. Gostiaux, H. Didelle, S. Mercier and T. Dauxois, *Exps. Fluids* **42**, 123–130 (2007).
8. B. Voisin, *J. Fluid Mech.* **496**, 243–293 (2003).
9. V. A. Gorodtsov and E. V. Teodorovich, *Fluid Dyn.* **17**, 893–898 (1982).
10. I. V. Sturova, *Fluid Dyn.* **36**, 478–488 (2001).
11. I. V. Sturova, *Fluid Dyn.* **41**, 619–628 (2006).
12. J. Lighthill, *Waves in Fluids* (Cambridge University Press, 1978), §4.10.
13. B. Voisin, Internal waves from oscillating objects, in *Proc. 6th Int. Symposium on Stratified Flows*, ed. G. N. Ivey (Perth, Australia, 2006), pp. 207–212.
14. D. G. Hurley, *J. Fluid Mech.* **351**, 105–118 (1997).
15. D. G. Hurley and G. Keady, *J. Fluid Mech.* **351**, 119–138 (1997).
16. D. G. Hurley and M. J. Hood, *J. Fluid Mech.* **433**, 61–75 (2001).
17. J. Happel and H. Brenner, *Low Reynolds Number Hydrodynamics*, 2nd edn. (Springer, 1983), Appendix A.
18. J. D. Jackson, *Classical Electrodynamics*, 3rd edn. (Wiley, 1999), §3.5.
19. P. M. Morse and H. Feshbach, *Methods of Theoretical Physics. Part II* (Feshbach Publishing, 1981), pp. 1295–1296.
20. J. C. Appleby and D. G. Crighton, *J. Fluid Mech.* **183**, 439–450 (1987).
21. J. C. Appleby and D. G. Crighton, *Q. J. Mech. Appl. Maths* **39**, 209–231 (1986).
22. L. D. Landau and E. M. Lifshitz, *Fluid Mechanics*, 2nd edn (Butterworth–Heinemann, 1987), §11.
23. J. Lighthill, *An Informal Introduction to Theoretical Fluid Mechanics* (Oxford University Press, 1986), §8.3.

24. Yu. Z. Miropol'skii, *Izv. Atmos. Ocean. Phys.* **14**, 673–679 (1978).
25. S. T. Simakov, *J. Fluid Mech.* **248**, 55–65 (1993).
26. J. N. Newman, *Adv. Appl. Mech.* **18**, 221–283 (1978).
27. R. Y. S. Lai and C.-M. Lee, *Int. J. Engng Sci.* **19**, 1411–1420 (1981).
28. L. H. Larsen, *Deep-Sea Res.* **16**, 587–603 (1969).
29. E. V. Ermanyuk, *Exps. Fluids* **28**, 152–159 (2000).
30. E. V. Ermanyuk and N. V. Gavrilov, *J. Fluid Mech.* **451**, 421–443 (2002).
31. E. V. Ermanyuk, *Exps. Fluids* **32**, 242–251 (2002).
32. E. V. Ermanyuk and N. V. Gavrilov, *J. Fluid Mech.* **494**, 33–50 (2003).
33. V. A. Gorodtsov and E. V. Teodorovich, *J. Appl. Mech. Tech. Phys.* **27**, 523–529 (1986).
34. J. Wu, *J. Fluid Mech.* **35**, 531–544 (1969).
35. C. P. Cerasoli, *J. Fluid Mech.* **86**, 247–271 (1978).
36. J. J. Riley, R. W. Metcalfe and M. A. Weissman, Direct numerical simulations of homogeneous turbulence in density-stratified fluids, in *Nonlinear Properties of Internal Waves*, ed. B. J. West, AIP Conf. Proc. No 76 (Am. Inst. Phys., 1981), pp. 79–112.
37. C. D. Winant, *Deep-Sea Res.* **21**, 445–453 (1974).
38. J. Cairns, W. Munk and C. Winant, *Deep-Sea Res.* **A26**, 369–381 (1979).